JOURNAL OF MATERIALS SCIENCE 23 (1988) 3326–3331

Raman study of alumina gels

T. ASSIH, A. AYRAL, M. ABENOZA, J. PHALIPPOU
Laboratoire de Science des Matériaux Vitreux, Université de Montpellier II, France

The sol–gel transition of an alumina sol is followed by Raman spectroscopy. Other spectroscopy techniques are also used to obtain additional information. The sol is made of particles of pseudo-boehmite which give rise to a Raman line at 360 cm^{-1}. The treatment of the sol by ethyl-ether extraction of 2-butanol confirms the presence of this band. Its assignment is made after a study of the spectra obtained during gelation on wet and dried gels. Raman spectroscopy does not show the presence of aluminium polycations in the sol. However, ^{27}Al nuclear magnetic resonance shows clearly the peak of the tetrahedrally coordinated aluminium atom located at the centre of these polycations. The presence of polycations contributes to explaining the slope change observed in the curve giving the Raman line intensities as a function of the aluminium content of the sample. X-ray diffraction and infrared spectroscopy enable us to correlate the Raman spectra of the gels heat-treated at various temperatures with respective structures.

1. Introduction

The synthesis of alumina from aluminium alkoxides is a promising way to prepare new ceramic compounds. The sol–gel process leads to high-purity powders and permits control of the morphology of the powders obtained [1]. Therefore a better control of the sintering stage is expected.

From this point of view a better knowledge of the different transformations occurring, from the chemical reactions involving the precursors to the final crystallization into α-Al_2O_3, is necessary.

Raman spectroscopy is a valuable tool for studying on a molecular scale the structural transformations which progressively occur during the sol-to-gel evolution and the subsequent thermal treatment of the gels. This technique has been extensively used in recent years for the study of silica sols and gels evolving towards glasses [2–10].

In the present work we have followed by Raman spectroscopy the structural evolution of peptized alumina sols as a function of the treatments which lead to α-alumina.

2. Experimental details

2.1. Sample preparation

The hydrolysis of aluminium secondary butoxide, $Al(OBu^s)_3$, was carried out by pouring the solution into water under vigorous stirring. The preparation is analogous to that reported by Yoldas [11]. Fig. 1 shows the flow chart of the whole sol–α-Al_2O_3 conversion.

Boehmite used as a reference sample was obtained by hydrothermal conversion of hydrargillite.

2.2. Experimental procedure

Raman spectra of sols and gels were recorded on a double-grating spectrometer using a Spectra Physics argon ion laser operating at 514.5 nm with 500 mW of power. The polarization of the incident light was carried out using a half-wave plate centred on 514.5 nm and that of scattering light, observed at 90°, using two other half-wave plates centred on 538 and 608 nm (850 and 2990 cm^{-1} from the excitation line). Typical spectra were recorded at 4 cm^{-1} resolution. A furnace specially adapted to the Raman set-up allowed us to obtain spectra during the gelation process; the temperature of the gel was controlled with an accuracy of 1° C.

Raman spectra of heat-treated gels were obtained by back-scattering from pellets using a T-800 Jobin Yvon triple monochromator associated with a Spectra Physics argon ion laser.

The structural characterization of the sol and wet gel was carried out using ^{27}Al nuclear magnetic resonance (NMR) spectroscopy. This technique enables the determination of the coordination of aluminium atoms. The spectra were obtained on a CXP 200 Bruker spectrometer (Service Commun de Résonance Magnétique Nucléaire de Matériaux Solides de l'USTL) working at 52 MHz under static conditions. The impulse time was 5 μsec and the duration between two impulses corresponded to 1 sec. The chemical shifts were evaluated from a standard saturated aqueous solution of aluminium chloride in which all aluminium atoms are in octahedral coordination $(Al(H_2O)_6)^{3+}$.

The structural evolution of the gel was also followed using infrared (IR) spectroscopy with the KBr pellet technique. Crystalline phases were identified using X-ray diffraction. The thermal behaviour of the gel was recorded by differential thermal analysis (DTA) with a heating rate of 13° C min^{-1}.

The turbidity of the sol was measured as a function of the concentration at a wavelength equal to that used to perform Raman spectroscopy.

0022–2461/88 $03.00 + .12

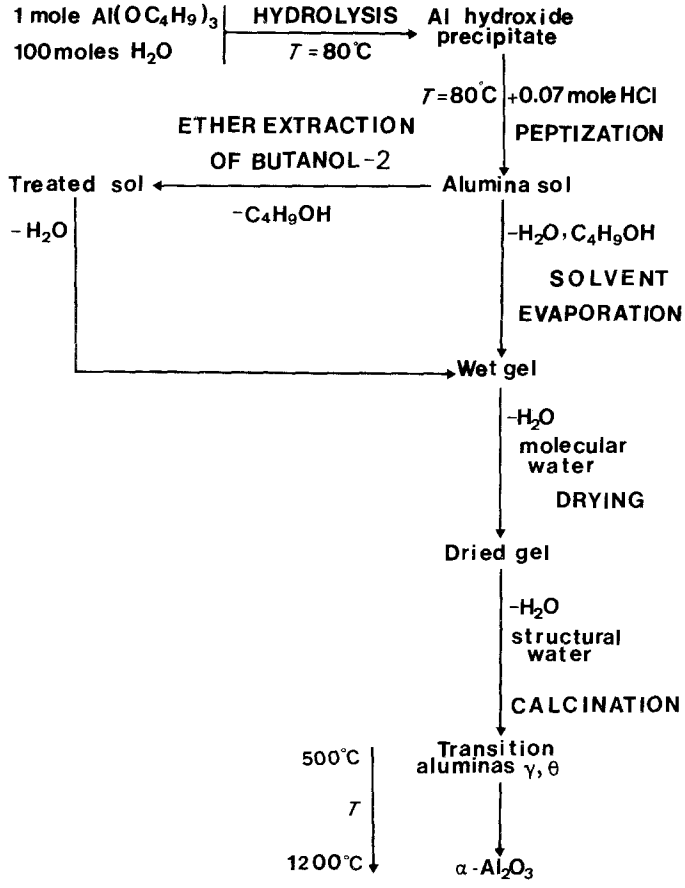

Figure 1 Flow diagram for processes used for the preparation of the materials.

3. Results and discussion

3.1. Study of the peptized sol

The spectrum of the peptized sol (Fig. 2c) includes all the lines of the 2-butanol (Fig. 2b) which is a by-product of the hydrolysis of the alkoxide. The intensity ratios of these lines are identical to those measured in pure 2-butanol. Typical lines of the alkoxide cannot be detected in the spectrum of the sol, and in particular the Raman line at 1060 cm^{-1} which is assigned to a stretching vibration of Al–O–C groups [12]. Thus the hydrolysis of the alkoxide is considered complete.

In addition, the spectrum of the sol shows a new band at 360 cm^{-1} which can be assigned to aluminium ions coordinated by six oxygen atoms [13]. This assumption has been confirmed by the study of sol after extraction of 2-butanol using ethyl-ether. In that case the spectrum of the treated sol (Fig. 2d) shows only the diffusion bands due to molecular water vibration (1600 cm^{-1}) and the band situated at 360 cm^{-1}, while the bands of 2-butanol have disappeared.

The sol has been analysed by ^{27}Al NMR. The spectrum (Fig. 3a) has been deconvoluted using a computer simulation. It appears to be constituted by three peaks. The peak situated between 60 and 70 p.p.m. is related to tetrahedral aluminium. The sharp peak around −7 p.p.m. and the other one near 0 p.p.m. are due to octahedral aluminium [14]. The most important feature of these spectra is the presence of a tetrahedral aluminium which was not detected by Raman spectroscopy. The aluminium atoms in fourfold coordination come from the polymeric aluminium cations. The pH of the sols is within the range 4 to 4.3. The presence of these kinds of cation has been demonstrated in the same range of pH [15]. ^{27}Al NMR shows that the central atom of the polycation $[Al_{13}O_4(OH)_{24}(H_2O)_{12}]^{7+}$ is in tetrahedral coordination [16]. The other twelve aluminium atoms which sur-

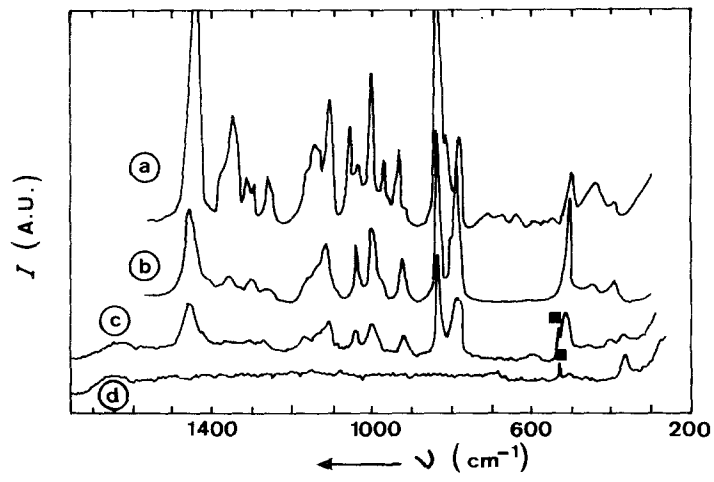

Figure 2 Raman spectra of (a) aluminium sec-butoxide, (b) 2-butanol, (c) untreated sol, (d) treated sol. A.U. = arbitrary units. (■) Laser peak.

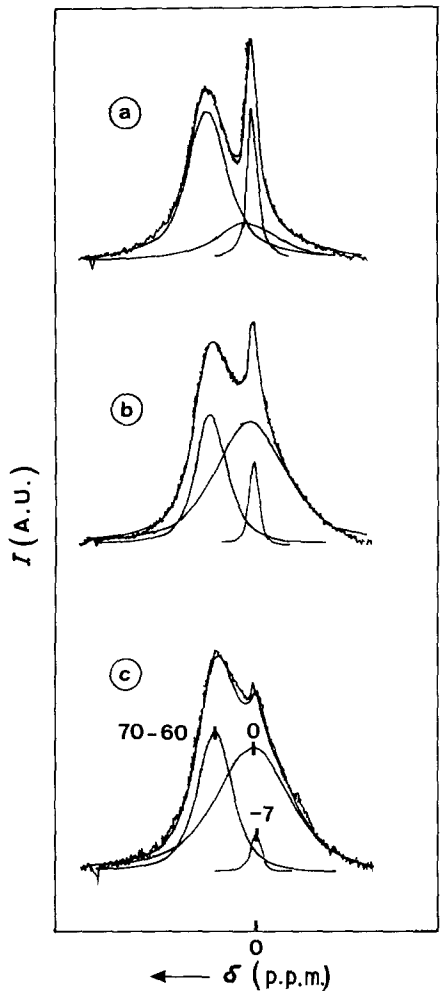

Figure 3 ^{27}Al NMR spectra of (a) tne initial sol (aluminium concentration C_0), (b) a concentrated sol (aluminium concentration C_1) and (c) a concentrated gel (aluminium concentration C_2), with $C_0 < C_1 < C_2$ (see Fig. 5).

round the aluminium mentioned above are in sixfold coordination. Due to their non-symmetrical environment they give rise to a peak too broad to be detected [16].

The sharp peak situated at -7 p.p.m. corresponds to aluminium linked with molecular water to form free $[Al(H_2O)_6]^{3+}$ ions. The broad peak centred at 0 p.p.m. is attributed to sixfold-coordinated aluminium atoms which correspond to those detected by Raman spectroscopy.

3.2. Study of the gelation of the sol

Gelation was induced by gently evaporating the solvent. The evaporation was carried out at a temperature of 70° C. Spectra were regularly recorded during the whole duration of the sol–gel transformation and then well after the gelation.

The evolution of Raman spectra as a function of aluminium concentration is shown in Fig. 4. Characteristic bands due to 2-butanol progressively disappear. It is worth noticing that the intensity of the 360 cm^{-1} band increases with the concentration of aluminium. At the same time new bands located at 451, 494 and 677 cm^{-1} emerge from the background of the spectrum.

The aluminium content of the sample is evaluated from the initial amount of aluminium ions introduced in the starting solution and from the volume occupied by the sol or gel as a function of the solvent evaporation. Fig. 5 shows that the intensity of the Raman lines varies with aluminium concentration. A change in the slopes is observed for an aluminium content corresponding to the concentration range where the sol–gel conversion occurs. This phenomenon cannot be attributed to a sudden change in the sample transmission (Fig. 6).

^{27}Al NMR was also used to follow the structural evolution as a function of the aluminium content of the sol and of the gel during the solvent evaporation treatment as well. Starting with an aluminium content C_0, the gelation approximately occurs for $C = 5C_0$. Fig. 3 shows the spectra obtained for various concentrations. For all the spectra, computer simulation confirms the presence and the position of the three peaks pointed out for the initial sol. However, when the aluminium content of the sol increases, the ratio of

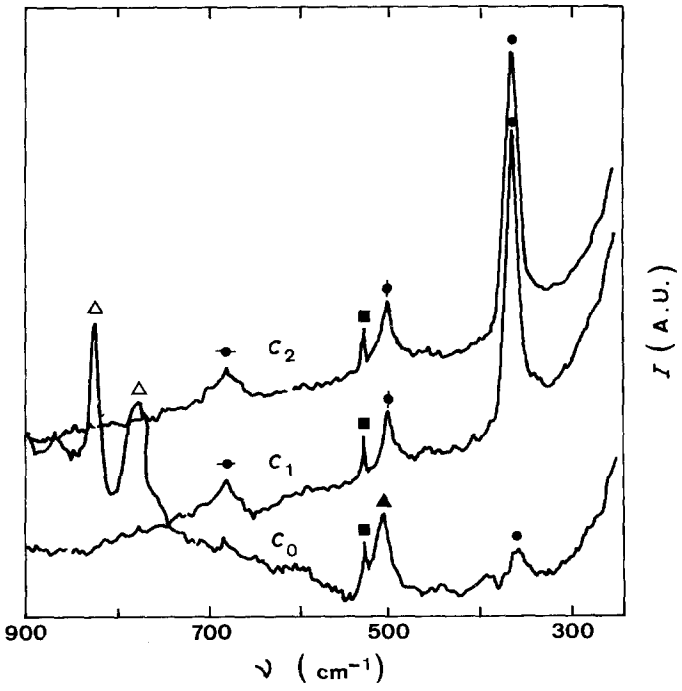

Figure 4 Evolution of the Raman spectra with aluminium concentration, $C_0 < C_1 < C_2$ (see Fig. 5). (●) Pseudo-boehmite, (△) 2-butanol, (■) laser.

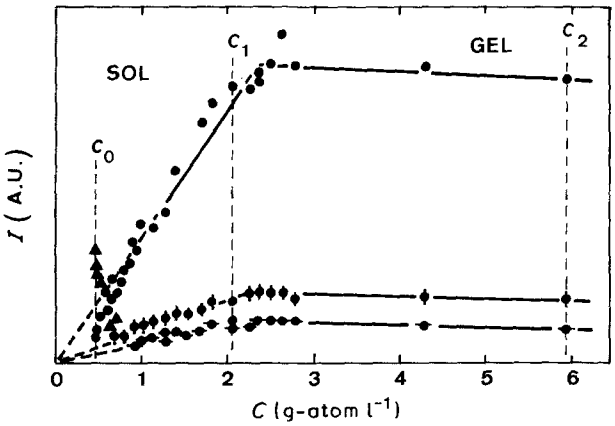

Figure 5 Raman line intensities against aluminium concentration (the lines followed are those marked in Fig. 4).

the area under the 0 p.p.m. peak to the area under the 60 to 70 p.p.m. peak is increased.

3.3. Structural characterization of the gel

The Raman spectrum of the dried gel is identical to that of the wet gel if the bands due to water are not taken into account. The dried gel displays a very strong 360 cm^{-1} Raman band. The other broad bands located at 451, 494 and 677 cm^{-1} are less intense. This spectrum is analogous to that of a polycrystalline boehmite sample AlO(OH) [13]. However, X-ray diffraction carried out on a dry powdered gel (Fig. 7) shows broad diffraction peaks. Moreover, the diffraction peak corresponding to 0 2 0 planes appears at a lower angle. Thus the sample is more probably made of pseudo-boehmite:

$$Al_2O_3 \cdot xH_2O \qquad 1.4 < x < 2$$

To the best of our knowledge, no Raman study has been performed on the pseudo-boehmite as yet. Table I reports the main characteristics (frequencies, width and intensity of the lines) of the spectra of a dried gel and of a boehmite sample. A comparison of the IR spectra of these two compounds is also given in Table I.

TABLE I Raman and infrared data for boehmite and dry alumina gels (ν_0 = frequency, $\Delta\nu$ = half-width, I = observed intensity in arbitrary units; w = weak, vw = very weak, sh = shoulder)

Raman spectra						IR spectra	
Boehmite			Dry gel			Boehmite	Dry gel
ν_0 (cm^{-1})	$\Delta\nu$ (cm^{-1})	I	ν_0 (cm^{-1})	$\Delta\nu$ (cm^{-1})	I	ν_0 (cm^{-1})	ν_0 (cm^{-1})
			324		vw	322	320
360	9	100	360	18	100	366	360
						395	
447	8	5	451	25	5		
						482	480
495	11	25	494	21	21		
						610	610
676	19	25	677	30	16		
						775	770
						1066	1070
						1155	1160
3065							
3084		sh	3087		w	3090	3090
3210		vw	3215		vw	3295	3300

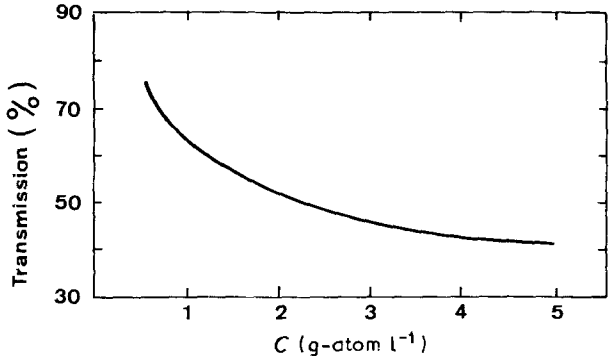

Figure 6 Transmission against aluminium concentration in the sol and gel (100% transmission for pure water).

The bands located at frequencies lower than 800 cm^{-1} are assigned to vibrations of AlO_6 groups [13, 17]. The relative intensities of Raman bands are identical for the two compounds.

The half-height widths of the bands are larger for the gel than for the boehmite sample. Thus, alumina gels are probably constituted by octahedral AlO_6 groups with a wide distribution of Al–O bond length and bond angle around mean values similar to those observed in boehmite.

In the frequency range corresponding to the stretching vibration of the OH group (3000 to 3800 cm^{-1}) the Raman spectrum confirms the above assumption. Although the literature reports, contradictory explanations [18–20], the Raman spectrum of boehmite indicates that the hydroxyl groups are linked by non-linear hydrogen bonds. These hydrogen bonds link the octahedral layers together. There are two equilibrium distances of the OH bonds which must be correlated to the two diffusion bands situated at 3065 and 3085 cm^{-1}. However, the spectrum of the pseudo-boehmite sample shows a single band in the same frequency range. Moreover, this diffusion band is less intense and very broad. The shape of the band indicates that the distribution of the OH bond length is very broad.

The broad peak centred on 0 p.p.m. which appears

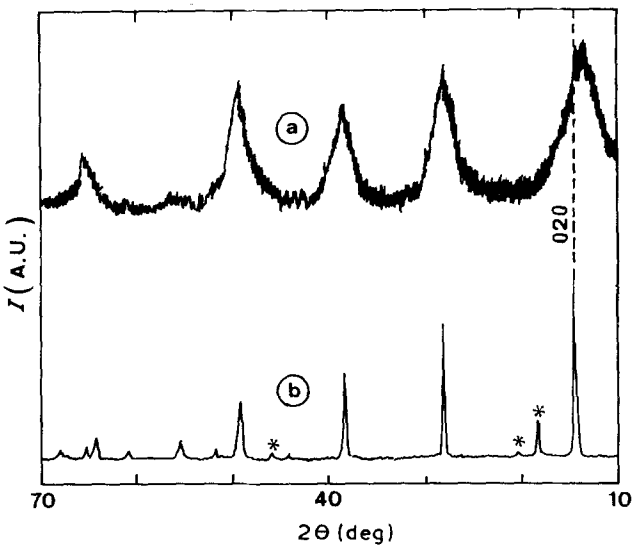

Figure 7 X-ray diffraction patterns of (a) dried gel and (b) stoichiometric boehmite; (*) residual hydrargillite.

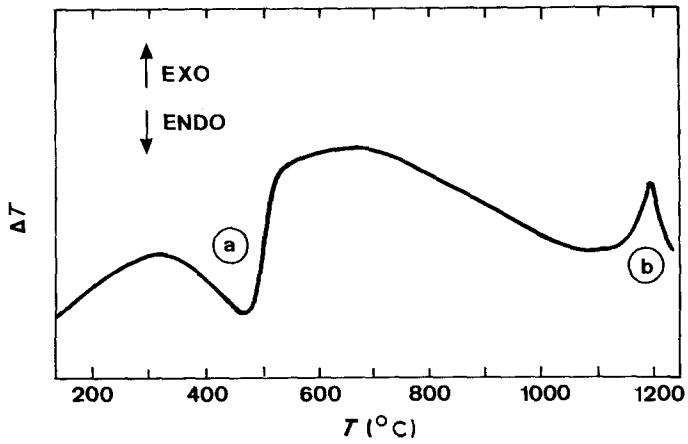

Figure 8 DTA curve of a dried gel (heating rate 13° C min^{-1}): (a) pseudo-boehmite → γ-Al_2O_3, (b) θ-Al_2O_3 → α-Al_2O_3.

on the ^{27}Al NMR spectra of sols and gels is assigned to the aluminium atoms of pseudo-boehmite particles. Polycations of aluminium are formed on the surface of the pseudo-boehmite during the peptization step. They cause the repulsion between the particles. During the sol–gel conversion the pseudo-boehmite compound forms at the expense of aluminium polycations. The mechanism by which this new pseudo-boehmite is created is not clear. It seems that the formation of pseudo-boehmite does not give rise to a significant increase of the particle size (from turbidity measurements). However, this transformation contributes to explaining the evolution of the Raman lines intensities with aluminium concentration.

3.4. Structural evolution with temperature

The dehydration of pseudo-boehmite and then its calcination give rise to the following crystallization sequence [21]:

Pseudo-boehmite → γ-Al_2O_3 → θ-Al_2O_3 → α-Al_2O_3

δ-Al_2O_3, which usually occurs immediately after γ-Al_2O_3 when heating boehmite, is not presently detected. This phenomenon must be linked to the porosity of the material [22].

DTA (Fig. 8) shows an endothermic peak situated at about 450° C corresponding to the pseudo-boehmite → γ-Al_2O_3 transformation. The exothermic peak at 1200° C refers to the well-known θ-Al_2O_3 → α-Al_2O_3 transformation.

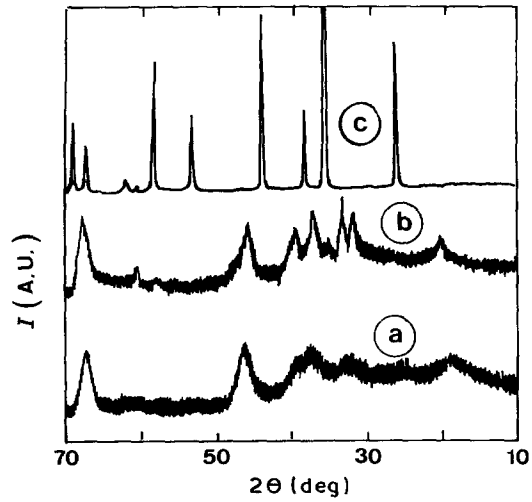

Figure 9 X-ray diffraction patterns of (a) γ-Al_2O_3, (b) θ-Al_2O_3 + γ-Al_2O_3, (c) α-Al_2O_3.

The temperature range of stability of the various transition aluminas has been determined using X-ray diffraction (Fig. 9). Gels were heat-treated for two hours at a given temperature. γ-Al_2O_3 is stable within a large temperature range. As reported in Table II, it was not possible to obtain pure θ-Al_2O_3. The material obtained after heat-treatment between 1000 and 1100° C mainly contains the θ phase but also another one (γ or α).

To the best of our knowledge there is no Raman spectroscopy study of transition aluminas. Raman diffusion spectra were therefore obtained to try to establish the structure of the atomic groups which are present in the different phases.

The Raman spectra obtained using a retrodiffusion set-up on compacted gels are shown in Fig. 10.

Corresponding IR spectra of the gels were also obtained. They exhibit poorly resolved absorption bands as previously reported [17, 23, 24]. Several remarks can be made:

(a) The spectrum of the gel heat-treated at 400° C is identical to that of the gel dried at room temperature. Thus the structure of pseudo-boehmite is stable up to 400° C. However, we have to notice that the frequency range studied does not allow the detection of other compounds such as molecular water or organic impurities.

(b) The γ-Al_2O_3 spectrum only shows very weak bands which are very broad. They are located at 480, 600 and 750 to 800 cm^{-1}. Identically, the IR spectrum shows three broad, poorly resolved bands at $\approx$400, 600, and 800 cm^{-1} which are considered as

TABLE II X-ray diffraction results for gels heated at various temperatures for two hours (Ps-B = pseudo-boehmite)

T (° C)	Phases
100	Ps-B
200	Ps-B
300	Ps-B
400	Ps-B
500	γ
600	γ
700	γ
800	γ
900	γ
1000	$\gamma + \theta$
1100	$\theta + \alpha$
1200	α

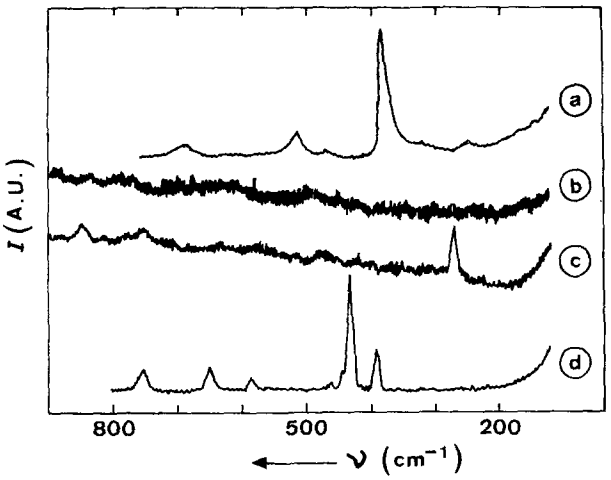

Figure 10 Raman spectra of (a) dried gel, (b) γ-Al_2O_3, (c) θ-Al_2O_3 ($-\gamma$-Al_2O_3), (d) α-Al_2O_3.

characteristic of γ-Al_2O_3 [24]. We can conclude that there is not a well-defined order around the aluminium ions and that a translational symmetry is missing. The pseudo-boehmite $\rightarrow$ γ-Al_2O_3 transformation probably occurs without a complete recrystallization phenomenon and by a rearrangement to a small extent of the various atoms. Raman and IR results confirm the assumption that γAl_2O_3 exhibits a deficient spinel structure [25]. In this kind of structure both octahedral and tetrahedral sites are observed for aluminium. However, the arrangement of atoms around the aluminimum is disordered. This structure leads to a breakdown of the selection rules, and as a consequence the spectrum shows weak and broad lines.

(c) The X-ray diffraction spectrum confirms that the gel heat-treated at 1000° C is constituted by γ and θ aluminas. The Raman spectrum of this sample shows a relatively intense line situated at 270 cm^{-1}. Some other very weak bands at 840, 750, 520, 460 and 400 cm^{-1} are also observed. The appearance of this new band at 270 cm^{-1} means that the $\gamma \rightarrow \theta$ transformation is accompanied by important atomic rearrangements. The most intense Raman bands are usually due to symmetrical vibrations which are located above 400 cm^{-1}. At this stage of the study the assignment of the 270 cm^{-1} band is not very clear.

(d) Raman and IR spectra of the gel heat-treated at 1200° C are similar to those of α-Al_2O_3. They show all the bands of the corundum compound [26] which is characterized by a very intense Raman line at 418 cm^{-1} and a well-defined IR band at 450 cm^{-1} [24].

4. Conclusions

Raman spectroscopy is a very efficient tool for the study of sols and gels. It has allowed us to determine, *in situ*, the structure of the colloidal particles. The structural evolution of the material has been followed continuously up to its term, anhydrous stable α-Al_2O_3.

Raman spectroscopy associated with ^{27}Al NMR spectroscopy has produced useful data on the complex organization of alumina sols and on the sol–gel transition.

In particular, ^{27}Al NMR has shown that the sol contains aluminium polycations which are adsorbed at the surfaces of colloidal pseudo-boehmite particles. These aluminium polycations can play a role in the stabilization of the sol, allowing the peptization phenomenon to occur.

Acknowledgements

The authors are grateful to Dr L. Seigneurin for kindly providing the boehmite sample. We wish to thank Drs P. Bernier, A. Whittaker (CNRS) for their help with the NMR experiments. Spectrum deconvolution was done using a program written by P. F. Barron.

References

1. A. AYRAL and J. PHALIPPOU, *Adv. Ceram. Mater.*, to be published.
2. A. BERTOLUZZA, C. FAGNANO, M. A. MORELLI, V. GOTTARDI and M. GUGLIELMI, *J. Non-Cryst. Solids* **48** (1982) 117.
3. V. GOTTARDI, M. GUGLIELMI, A. BERTOLUZZA, C. FAGNANO and M. A. MORELLI, *ibid.* **63** (1984) 71.
4. D. M. KROL and J. G. VAN LIEROP, *ibid.* **63**, (1984) 131.
5. L. C. KLEIN, C. NELSON and K. L. HIGGINS, *Mater. Res. Soc. Symp. Proc* **32** (1984) 293.
6. T. W. ZERDA, M. BRADLEY and J. JONAS, *Mater. Lett.* **3** (1985) 124.
7. I. ARTAKI, M. BRADLEY, T. W. ZERDA and J. JONAS, *J. Phys. Chem.* **89** (1985) 4399.
8. I. ARTAKI, T. W. ZERDA and J. JONAS, *J. Non-Cryst. Solids* **81** (1986) 381.
9. D. M. KROL, C. A. MULDER and J. G. van LIEROP, *ibid.* **86** (1986) 241.
10. I. ARTAKI, M. BRADLEY, T. W. ZERDA, J. JONAS, G. ORCEL and L. L. HENCH, in "Science of Ceramic Chemical Processing", edited by L. L. Hench and D. R. Ulrich (Wiley, New York, 1986) p. 73.
11. B. E. YOLDAS, *Bull. Amer. Ceram. Soc.* **54**(3) (1985) 289.
12. D. L. GUERTIN, S. E. WIBERLEY, W. H. BAUER and J. GOLDENSON, *J. Phys. Chem.* **60** (1956) 1018.
13. A. B. KISS, G. KERESZTURY and L. FARKAS, *Spectrochim. Acta* **36A** (1980) 653.
14. S. KOMARNENI, R. ROY, C. A. FYFE and G. J. KENNEDY, *J. Amer. Ceram. Soc.* **68** (1985) C243.
15. J. Y. BOTTERO, J. M. CASES, F. FIESSINGER and J. E. POIRIER, *J. Phys. Chem.* **84** (1980) 2933.
16. J. Y. BOTTERO, J. M. CASES, P. RUBINI and F. FIESSINGER, *C.R. Acad. Sci. Paris* **284D** (1977) 1033.
17. M. C. STEGMANN, D. VIVIEN and C. MAZIERES, *Spectrochim. Acta* **29A** (1973) 1653.
18. V. C. FARMER, *ibid.* **36A** (1980) 585.
19. A. B. KISS, P. GADO and G. KERESZTURY, *ibid.* **38A** (1982) 1231.
20. P. G. MARDILOVITCH and A. I. TROKHIMETS, *Zh. Prikl. Spektrosk.* **36** (1982) 258.
21. T. SATO, *Z. Anorg. Chem.* **391** (1972) 167.
22. B. C. LIPPENS and J. H. de BOER, *Acta Crystallogr.* **17** (1962) 1312.
23. D. E. CLARK and J. J. LANNUTTI, in "Ultrastructure Processing of Ceramics, Glasses and Composites", edited by L. L. Hench and D. R. Ulrich (Wiley, New York, 1984) p. 126.
24. P. P. MARDILOVITCH, A. I. TROKHIMETS and M. V. ZARETSKII, *Zh. Prikl. Spectrosk.* **40** (1984) 409.
25. M. C. STEGMANN, D. VIVIEN and C. MAZIERES, *J. Chim. Physique* **71** (1974) 761.
26. S. P. S. PORTO and R. S. KRISHNAN, *J. Chem. Phys.* **47** (1967) 1009.

Received 24 September 1987
and accepted 26 January 1988